CHEMMEDCHEM

DOI: 10.1002/cmdc.200700349

Herceptin–Platinum(II) Binding Complexes: Novel Cancer-Cell-Specific Agents

Jian Gao,*[a, b] Ya Guang Liu,[b] Renbin Liu,[c] and Ralph A. Zingaro*[a]

We report a new series of Herceptin–platinum(II) binding complexes, Her–nLPt^{II} (Her denotes Herceptin; L denotes diamino ligands and L = L1–L4; n = 1, 5, or 10). Solution chemistry studies have shown that these complexes are stable under physiological conditions (pH 7.4 in PBS). The platinum(II) compound L1$Pt^{II}Cl_2$ inhibits the growth of a panel of human cancer cell lines at submicromolar concentrations. Remarkable cancer-cell-specific cytotoxicity was observed with Her–nL1Pt^{II} (n = 1, 5, 10) toward Her2/neu-overexpressing cancer cells (SK-BR-3 and SK-OV-3) over normal fibroblast cells. Annexin V apoptosis assays in SK-BR-3 and low-Her2/neu-expressing MCF-7 breast cancer cells further confirmed the critical role of Herceptin with this cancer-cell-specific agent. It was also found that the L1$Pt^{II}Cl_2$ complex is an efficient regulator of the apoptotic genes Bcl-2 in the treated SK-BR-3 cells. Also, enhanced regulatory effects were observed in Her–10L1Pt^{II}. Taken together, this study suggests a new approach for the development of mAb–platinum(II)-based targeting agents for the treatment of human cancers.

Introduction

The development of cancer-cell-specific drug motifs is critical in the treatment of human cancers.[1,2] During the last decade, a variety of drug carriers such as nanosized devices, which are capable of targeting tumor tissue have been developed.[3,4] However the tumor-cell specificity in vivo and biodegradability of the carriers that are in current use require significant improvements. Furthermore, the minimization of negative side-effects of such methodologies is of critical importance. Over the past few years, targeted anticancer agents, which were constructed by coupling cell-membrane-specific molecules and cytotoxic agents through bioconjugation have attracted considerable attention.[5,6] Of this approach, a variety of macromolecules and small biomolecules have been employed. Monoclonal antibodies that possess high binding affinity to overexpressed proteins in cancer cells have been shown to be one of the primary targeting agent.[7–9]

Herceptin (also known as tratuzumab) is an FDA-approved humanized monoclonal antibody (mAb) and has been shown to be one of the most useful biological agents for the treatment of breast cancer.[10] It binds to the Her2/neu protein, which is a member of the epidermal growth factor receptor family (EGFR, also known as ErbB) of receptor tyrosine kinases. Herceptin's inhibition of tumor cell growth depends largely on its binding action, and is currently in use as a treatment for Her2/neu-overexpressing breast cancer.[11] According to the American Cancer Society, 25–30% of patients overexpress Her2/neu, and can potentially benefit from treatment with Herceptin. Although it represents a useful biological approach, Herceptin has also been combined with chemotherapeutic agents to increase its therapeutic utility.[12]

In general, mAbs are more specific than small molecules to targeted cancer cells, but small molecules can achieve higher levels of cytotoxicity. Our interest in this study arises from the potential of combining mAb with a synthetic agent, and how the resulting complex differs from the individuals in terms of cancer cell specificity and toxicity. We report herein a chemical and biological study of new Herceptin–platinum(II) complexes, Her–*n*LPt^{II} (*n* = 1, 5, and 10, L = L1, L2, and L3) that display remarkable tumor cell selectivity to Her2/neu- overexpressing cancer cell lines. It is demonstrated that the specificity and toxicity to SK-BR-3 cells both increase with the increment of the number (*n* value) in the complex. The annexin V apoptosis assay substantiated the observed cancer-cell-specific effect of the complexes in tested cell lines. It is also reported that L1$Pt^{II}Cl_2$ is effective in the down regulation of the expression of the apoptosis-related gene Bcl-2 in SK-BR-3 cells. A pronounced down regulation of Bcl-2 was observed for Her–10L1Pt^{II} at the same concentration.

[a] *Prof. J. Gao, Prof. R. A. Zingaro*
Department of Chemistry, Texas A&M University
College Station, TX 77843-3255 (USA)
Fax: (+1) 210-372-0896 (J.G.)
(+1) 979-845-2731 (R.A.Z.)
E-mail: gaojiantamu@yahoo.com
Zingaro@mail.chem.tamu.edu

[b] *Prof. J. Gao, Y. G. Liu*[+]
School of Medicine, University of Texas Health Science Center
San Antonio, TX 78229-3900 (USA)

[c] *Prof. R. Liu*[+]
The First Affiliated Hospital
Sun Yat-Sen University, Guang Zhou, 510080 (P. R. China)

[+] *These authors contributed equally to this work.*

Supporting information for this article is available on the WWW under http://www.chemmedchem.org or from the author.

Results

Synthesis of Pt^{II}-based compounds

Compounds L1–L3 were synthesized by Schiff-base condensation between diaminocyclohexane (DACH) and 2-hydroxy-5-methylsalicylaldehyde, followed by reductive hydrogenation (Figure 1). The crude products were purified by silica gel

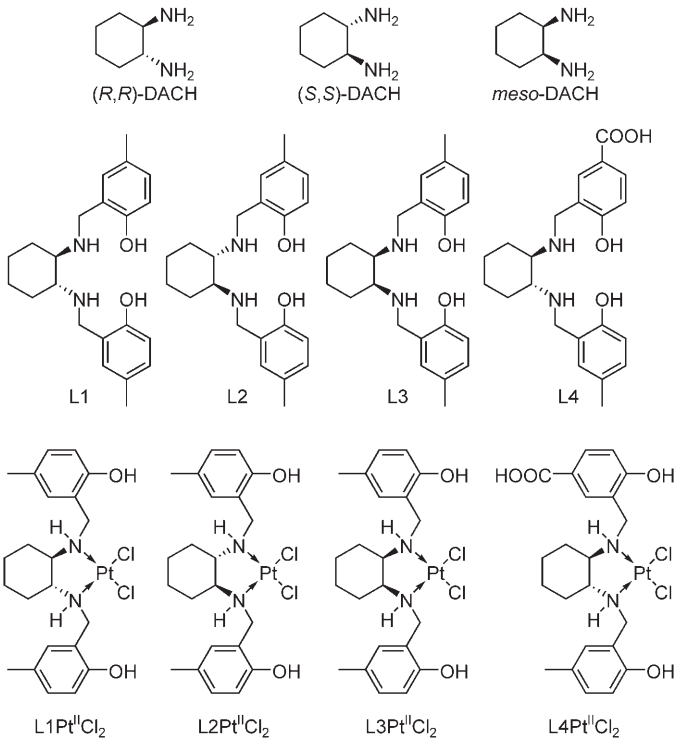

Figure 1. Building blocks and molecular structures of the compounds synthesized.

column chromatography, and the diamino compounds were obtained in high yield (> 80%). L4 was synthesized by a similar approach from an equimolar amount of (*R*,*R*)-DACH, 2-hydroxy-5-methylsalicylaldehyde, and 2-hydroxy-5-carboxysalicylaldehyde in the presence of 3 equiv triethylamine. This compound was purified by silica gel column chromatography (H_2O/MeOH/CH_2Cl_2 1:3:16). The diamino building blocks are all possible stereoisomers of DACH, which allowed us to observe isomer preference in the in vitro phase study. The platinum(II) complexes $LPt^{II}Cl_2$ (L = L1–L4) were successfully prepared by the direct reaction of the ligands with K_2PtCl_4 in a solution of MeOH/H_2O.

Characterization of Her–*n*LPt^{II} binding complexes

The binding complexes were synthesized by treating a series of aqueous solutions that contained 1.0×10^{-3} mmol of Herceptin antibody with 1, 5, 10 and 20 equiv compound $L1Pt^{II}Cl_2$. The resulting solutions are homogeneous at room temperature, and no precipitates formed during the next two hours. The binding complex solutions were filtered by size-exclusion chromatography (5000 Da). Because Herceptin is a 175-kDa macromolecule, a direct analysis of the number of binding small molecules is difficult. However, analysis of the component in the filtrate is a possible way to monitor the binding ratio of platinum complex to the protein.

To this end, the filtrate was analyzed by UV/Vis spectroscopy in the range of 200–500 nm to monitor the unbound platinum compounds. Figure 2A shows the absorption spectrum of K_2PtCl_4, L1 and neat $L1Pt^{II}Cl_2$ solution at 1.0 mM concentration. In the control experiment, the filtrate of 1.0 mM aqueous Herceptin solution was measured, and no absorption could be observed in the tested range. A comparison of these absorption curves shows that the absorption maximum at 273 nm is diagnostic for $L1Pt^{II}Cl_2$. The extinction coefficient measured for $L1Pt^{II}$ is 2.99×10^3 mM cm^{-1} (Supporting Information). As shown in Figure 2B, each of the filtrates was measured over the same range, and all the samples showed a similar absorption spectrum, but with decreased absorbance at 273 nm. The concentrations of the unattached platinum compound were determined by establishing a standard curve for $L1Pt^{II}Cl_2$, and the percentage of $L1Pt^{II}Cl_2$ that was bound to Herceptin is shown in Figure 2C.

In the second set of experiments, the stability of the binding complexes was evaluated. The luminescence-tagged compound $L5Pt^{II}Cl_2$ (Figure 3) was prepared and it was applied in the preparation of the Herceptin binding complexes by following a procedure as described above. Fluorescent emission spectra for neat $L5Pt^{II}Cl_2$ and the corresponding binding complexes Her–*n*$L5Pt^{II}$ (*n* = 1, 5, and 10) are shown in Figure 2D, These results show that only a trace amount of the organic ligand (L5) could be detected in the filtrate.

Subsequently, the stability of the binding complexes under different pH conditions was investigated. In general, metal complexes can interact with a protein molecule noncovalently or by coordination. The binding complex Her–10$L1Pt^{II}$, which is stable at pH 7.4, was found to undergo dissociation in acidic solution. The dissociation behavior of the complex was monitored spectrophotometrically (Figure 2E). In each of the tested pH values, the filtrate of the acidified sample solution was measured. The variation of absorption maximum at 273 nm indicated that Her–10$L1Pt^{II}$ started to dissociate from Herceptin at pH 7.0, and was fully dissociated at pH 4.8. The phenomenon explicitly illustrates the critical role that protons play in the reversible binding of $L1Pt^{II}Cl_2$ with Herceptin.

In vitro anticancer activities of $LPt^{II}Cl_2$ (L = L1–L3)

Initially, the cytotoxicity of compounds $L1Pt^{II}Cl_2$, $L2Pt^{II}Cl_2$ and $L3Pt^{II}Cl_2$ were tested against a panel of human cancer cell lines, including breast (SK-BR-3, MDA-MB-231), ovarian (SK-OV-3) and prostate (LNCap). These compounds were screened over a range of 100–0.01 μM (5-log dose range) concentrations. It was found that the compound with the (*R*,*R*)-diaminodiphenol scaffold, $L1Pt^{II}Cl_2$ possesses the highest cytotoxicity, and induces growth inhibition of all the cell types at the micromolar level (Figure 4A). The cytotoxicity of $L1Pt^{II}Cl_2$ was also evaluated in fibroblast cells, and is 30% less toxic toward normal cells

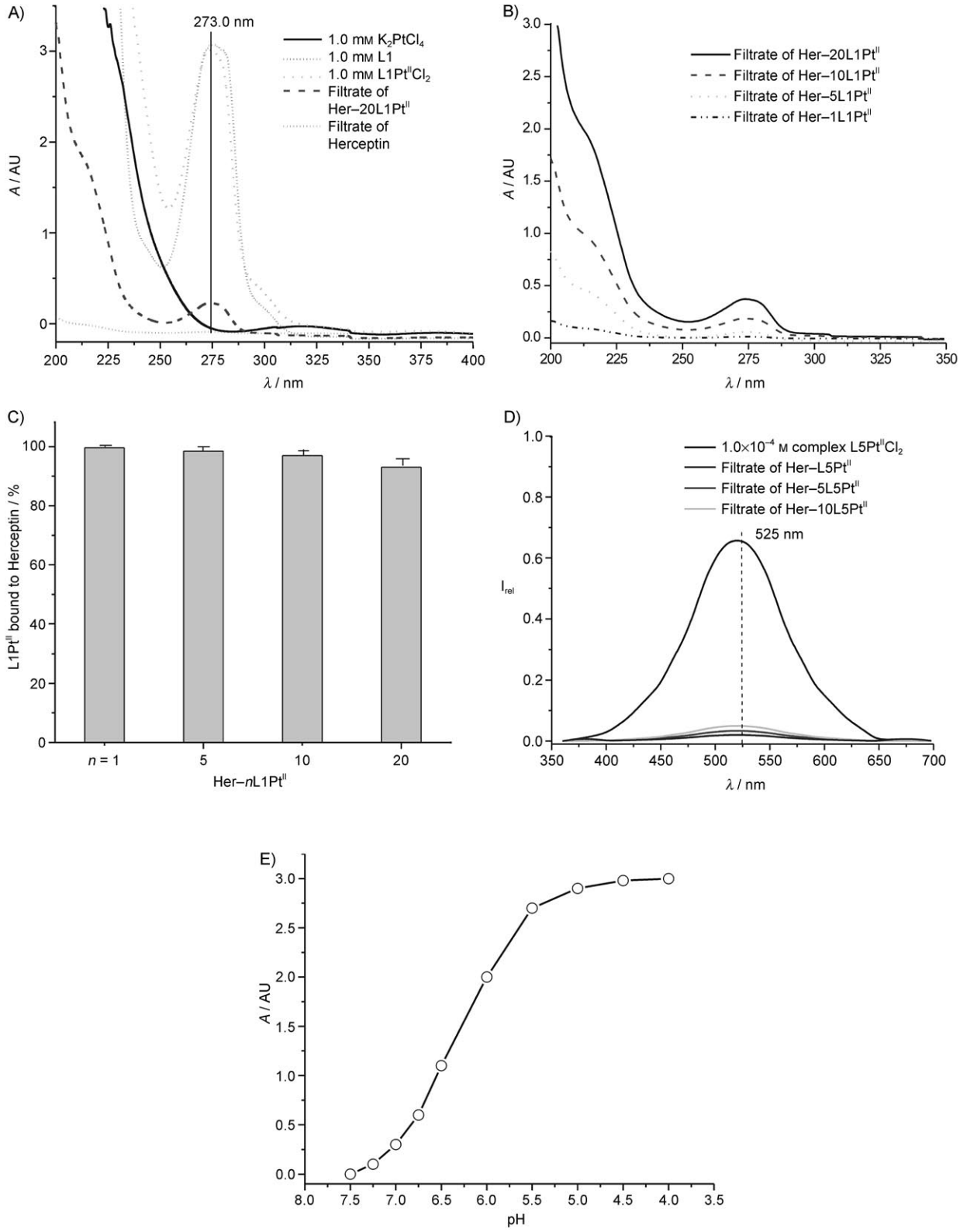

Figure 2. A) Absorption spectra of 1.0 mM K_2PtCl_4, L1, $L1Pt^{II}Cl_2$, Herceptin, and the filtrate of 1.0 mM binding complex Her–20L1Pt^{II}, which was separated by size-exclusion chromatography. B) Absorption spectra of binding complex filtrates of the various ratios indicated. C) Percentage of $L1Pt^{II}Cl_2$ bound to Herceptin in Her–*n*L1Pt^{II} as determined by calculation from the standard curve (A_{max} at $\lambda = 273$ nm). D) Fluorescence emission spectra of $L5Pt^{II}Cl_2$ (1.0×10^{-4} M) and the filtrates of Herceptin binding complexes at various ratios. E) Spectrophotometric determination of $L1Pt^{II}Cl_2$ dissociation from the Her–10L1Pt^{II} complex as a function of pH; [Her–10L1Pt^{II}] = 0.1 mM, and the absorption was monitored at 273 nm.

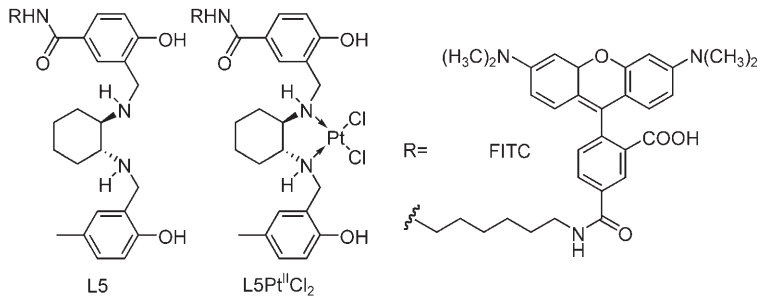

Figure 3. Fluorescein isothiocyanate (FITC)–ligand–Pt conjugates.

than toward cancer cells. This result clearly shows the ability of compound L1Pt^{II}Cl$_2$ to inhibit the growth of several major cancers. The IC_{50} values that were observed for compound L1Pt^{II}Cl$_2$ (Table 1) fall in the range of 1–10 μM. This compound is more promising than its *R*,*S* and *S*,*S* counterparts.

Table 1. Inhibition constants for Pt^{II}Cl$_2$ compounds.[a]

Cell line	IC_{50} [μM]		
	L1Pt^{II}Cl$_2$	L2Pt^{II}Cl$_2$	L3Pt^{II}Cl$_2$
SK-BR-3	2.8 ± 0.1	3.1 ± 0.1	3.1 ± 0.1
MDA-MB-231	1.2 ± 0.2	1.8 ± 0.2	2.1 ± 0.2
SK-OV-3	6.0 ± 0.1	6.4 ± 0.1	6.9 ± 0.1
LNCap	2.4 ± 0.1	2.5 ± 0.1	2.8 ± 0.2

[a] Mean of two experiments ± range.

The toxic effects of compound L1Pt^{II}Cl$_2$ were further validated in additional breast cancer cell lines MCF-7, T-47D and AU-565, which express Her2/neu at low levels. The degree of cell survival at a compound concentration of 2.5 μM is displayed in Figure 4B. It should be noted that compound L1Pt^{II}Cl$_2$ was more active toward Her2/neu-overexpressing cancer cells, SK-BR-3 and MDA-MB-231. For example, at the concentration levels tested, compound L1Pt^{II}Cl$_2$ inhibited cell growth by 38% in MCF-7, and induced 51% and 63% growth inhibition for SK-BR-3 and MDA-MB-231, respectively.

Cancer-cell-specific effects of Pt^{II}–Her complexes

To determine the cytotoxicity and specificity of Her–*n*L1Pt^{II}, cultured breast cancer cells SK-Br-3 and wild-type fibroblasts were treated concurrently with Her–*n*L1Pt^{II} ($n = 1$, 5, or 10). Initially the 1:1 binding complex, Her–L1Pt^{II} was used. The percentage of cell survival at a complex concentration of 5 μM for SK-BR-3 and WTF was 56.8% and 95.8%, respectively (Figure 5A). It was reasoned that increasing the ratio of platinum(II) compounds to Herceptin in the binding complex might increase the toxicity, or decrease the amount of Herceptin required. Because it is anticipated that the binding capacity of Herceptin does not decrease upon binding with multiple platinum compounds, increased tumor cell selectivity should be expected. To this end, Her–5L1Pt^{II} was tested against SK-BR-3 and fibroblasts. As shown in Figure 5B, Her–5L1Pt^{II} shows increased selectivity at 1.0 μM concentration. The percentage of cells that survived for SK-BR-3 and fibroblast is 42.6% and 93.7%, respectively.

Based on this success, it was decided to further test a higher-ratio platinum(II)–Herceptin complex, Her–10L1Pt^{II}. A more pronounced cancer cell line specificity was observed (Figure 5C). At a 1.0 μM concentration, the percentage of cells that survived for SK-BR-3 and fibroblast is 4.0% and 63.2%. Her–10L1Pt^{II} displayed a 16-fold greater sensitivity toward SK-BR-3 cells over normal cells. In addition, the cytotoxicity of the Herceptin antibody on SK-BR-3 and normal cells was investigated. It was noted that Herceptin induced only 15% growth inhibition of cancer cells at 1.0 μM (Figure 5D). These results indicate that the new binding motif represents a new type of potential targeting agents that are able to significantly increase the cytotoxicity toward cancer cells and spare the normal cells. The toxic effects of Her–10L1Pt^{II} were further evaluated in MCF-7 cells, but no selectivity was observed in the

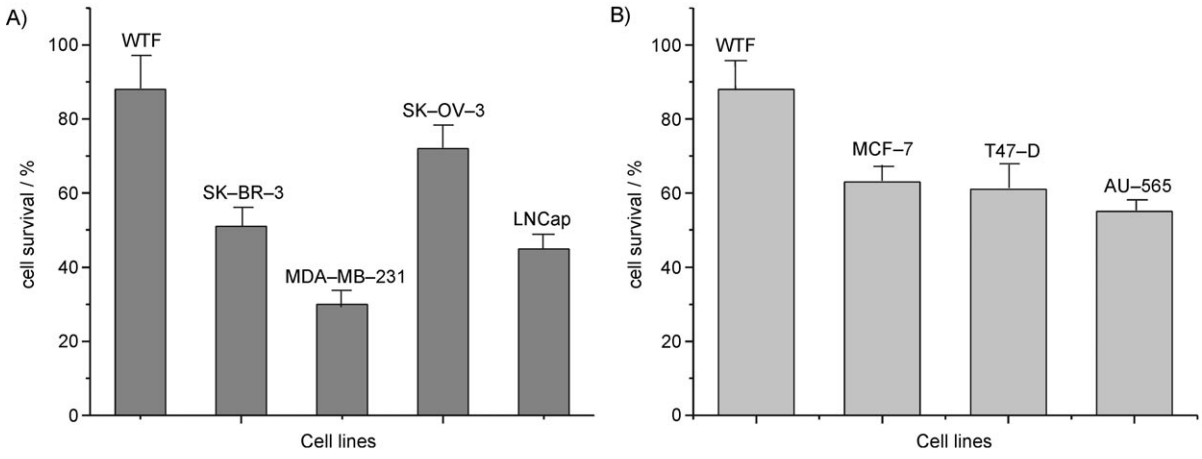

Figure 4. A) Growth-inhibitory effects of L1Pt^{II}Cl$_2$ toward a panel of human cancer cells; the cells were treated at 2.5 μM for 24 h, and the cells that survived were measured by SRB assay. B) Growth-inhibitory effects of L1Pt^{II}Cl$_2$ (2.5 μM) toward additional breast cancer cells, MCF-7, T-47D, and AU-565. (WTF = wild-type fibroblast cells).

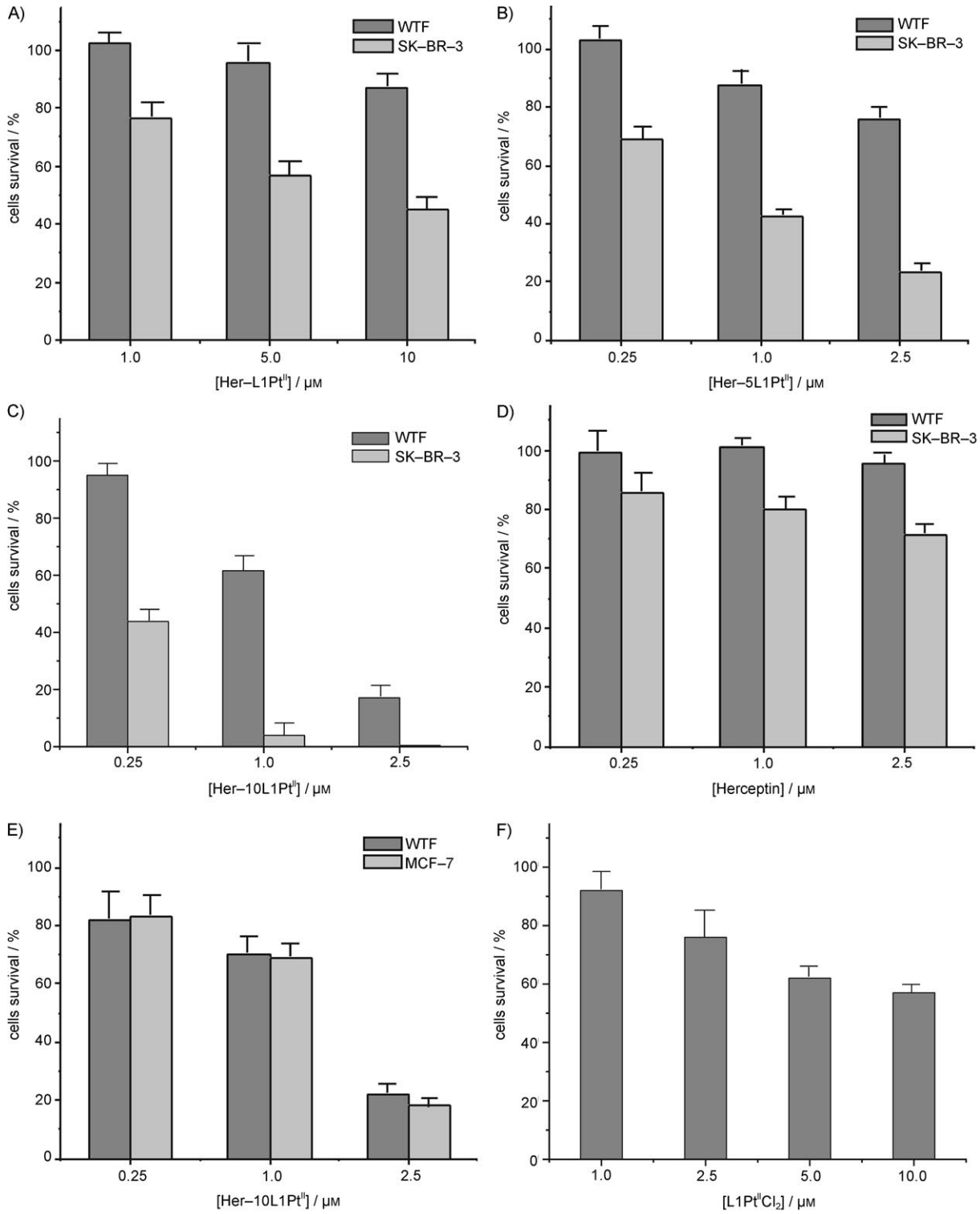

Figure 5. A) Growth-inhibitory effects of Her–L1Pt^{II} toward SK-BR-3 and normal (WTF) cells; the cells were treated at 1.0, 5.0, and 10.0 μM for 24 h, and the cells that survived were measured by SRB assay. B) Growth-inhibitory effects of Her–5L1Pt^{II} toward SK-BR-3 and normal cells; the cells were treated at 0.25, 1.0, and 2.5 μM for 24 h. C) Growth-inhibitory effects of Her–10L1Pt^{II} toward SK-BR-3 and normal cells; the cells were treated at 0.25, 1.0, and 2.5 μM for 24 h. D) Growth-inhibitory effects of Herceptin antibody toward SK-BR-3 and normal cells; the cells were treated at 0.25, 1.0, and 2.5 μM for 24 h. E) Growth-inhibitory effects of Her–10L1Pt^{II} toward MCF-7 and normal cells; the cells were treated at 0.25, 1.0, and 2.5 μM for 24 h. F) Growth-inhibitory effects of L1Pt^{II}Cl$_2$ toward MCF-7; cells were treated at 1.0, 2.5, 5.0, and 10.0 μM for 24 h.

tested range of concentration (Figure 5E). Taken together, Her–10L1Pt^{II} appears to be a highly specific anticancer agent toward Her2/neu-overexpressing cells.

Apoptosis assay for L1Pt^{II}Cl$_2$ and Her–10L1Pt^{II} in SK-BR-3 and MCF-7 cells

To confirm that the selective cytotoxicity in Her2/neu-overexpressing cells is caused by the Herceptin–Her2/neu interaction, SK-BR-3 cells were stained with annexin V–FITC and propidium iodide (PI) and analyzed by flow cytometry. As shown in Figure 6A, a dose-dependent induction of apoptosis was observed. The addition of L1Pt^{II}Cl$_2$ at a concentration of 0.5 μM resulted in 17% of the cells undergoing the early phases of apoptosis, compared with the lower level of apoptosis (10%) in untreated SK-BR-3 cells (quadrant 4), whereas 5.0 μM of L1Pt^{II}Cl$_2$ caused a 2.5-fold (25.5%) increase of apoptotic cells. Significantly, 0.5 μM Her–10L1Pt^{II} induced a pronounced rate of cells undergoing apoptosis (31.1%). A modest increase in the portion of apoptotic cells (33.04%) was observed for cells that were treated with 1.0 μM Her–10L1Pt^{II}; this suggests that there exist a limited number of Her2/neu receptors on the cell surface.

To obtain a further understanding of the critical role of Herceptin in the cancer-cell-specific agents, cultured MCF-7 cells were also assessed by an annexin V–FITC and PI binding assay. As shown in Figure 6B, the addition of a low-dose level (0.5 μM) of L1Pt^{II}Cl$_2$ induces a low level of apoptosis (quadrant 4, 2.79%) in MCF-7 cells compared with the very similar rate of spontaneous apoptosis of untreated control (2.25%); this indicates that L1Pt^{II}Cl$_2$ is less toxic at a low nanomolar level concentration. Herceptin antibody at a concentration of 0.5 μM resulted in a fourfold (8.28%) increase in the number of cells in the early phase of apoptosis. Whereas Her–10L1Pt^{II} (0.5 μM) induced a similar level of apoptosis (8.05%). These results indicate that binding with 10-fold excess of platinum molecules to one Herceptin does not increase the toxic effect of Herceptin toward cells that express a low level of Her2/neu proteins. In other words, Her–10L1Pt^{II} exclusively recognizes Her2/neu-expressing cancer cells.

Inhibition of apoptotic mRNA expression

Because of the profound cell-growth inhibition that was exhibited by the reported compounds, their effectiveness in regulating the expression of Bcl-2 family genes was tested. To deter-

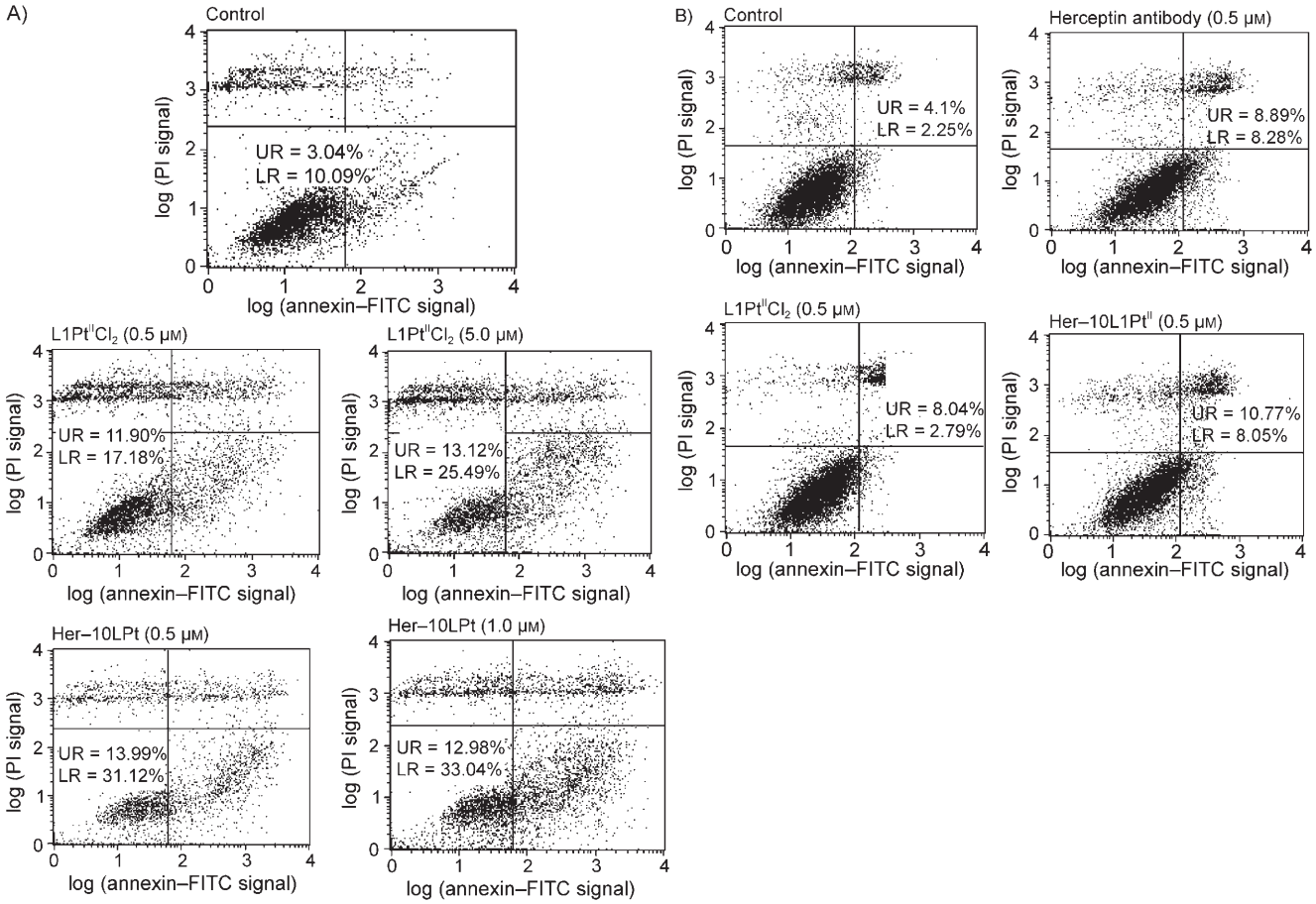

Figure 6. A) Compound L1Pt^{II} and Her–10L1Pt^{II} induce apoptosis in SK-BR-3 cells; cells were treated with L1Pt^{II} or Her–10L1Pt^{II} at the indicated concentrations for 20 h and were then stained with annexin V–FITC and PI, and analyzed by FACScan. B) Compound L1Pt^{II}, Herceptin, and Her–10L1Pt^{II} induce apoptosis in MCF-7 cells; cells were treated with L1Pt^{II}, Herceptin, or Her–10L1Pt^{II} at the indicated concentrations for 20 h and were then stained by annexin V–FITC and PI, and analyzed by FACScan. (UR = upper-right quadrant, LR = lower-right quadrant; percentages indicated gating threshold.)

mine the effects of complexes $L1Pt^{II}Cl_2$ on endogenous Bcl-2 mRNA expression, the amount of Bcl-2 mRNA expression in each sample was determined by real time RT-PCR. As shown in Figure 7, $L1Pt^{II}Cl_2$ down-regulates Bcl-2 mRNA expression up to

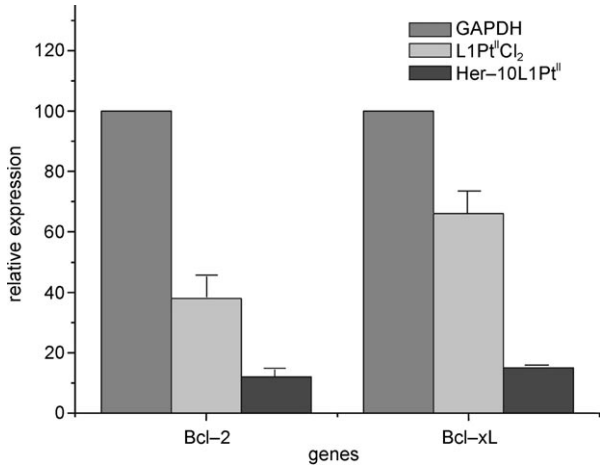

Figure 7. Relative expression of cell-cycle- and apoptosis-related genes. SK-BR-3 cells were treated with 2.5 μM $L1Pt^{II}Cl_2$ and Her–$10L1Pt^{II}$ for 20 h. Bcl-2 and Bcl-xL mRNA expression was determined by real-time RT-PCR and normalized with GAPDH expression in each sample.

62% compared with the untreated cells, and Her–$10L1Pt^{II}$ decreased the expression to 12% of the level of the untreated cells. The antiapoptotic gene Bcl-xL was also examined and $L1Pt^{II}Cl_2$ and Her–$10L1Pt^{II}$ were found to repress the expression of Bcl-xL to 66% and 15% of the level of control. These results indicate that the platinum(II)–Herceptin complexes effectively regulate the expression of cell apoptotic genes.

Discussion

Unlike organic molecules, metal-based chemical agents can achieve high binding affinity upon interaction with an antibody. This property has prompted the investigation of the compounds reported herein. The goal is to combine these compounds with Herceptin antibody. This approach may obviate the need for the preparation of mAb–drug conjugates, which might be more complex and difficult to develop as drugs. It is generally agreed that protein–protein interactions occur by hot spot binding.[13] The platinum(II) compound might bind randomly on the backbone of Herceptin and leave the hot spot intact. In fact, the platinum compound is not particularly designed to block protein–protein (Herceptin–Her2/neu) interactions. In this situation, the platinum(II)–Herceptin-binding complex might retain its capacity to recognize Her2/neu-overexpressing cells. This allows sensitive discrimination between targeted and normal tissues.

The newly synthesized Her–nLPt^{II} complexes differ from those that have been previously developed that use a conjugation strategy.[14] The conjugates are constructed by coupling monoclonal antibodies to drug molecules by a covalent bond. The stability of the links and the difficulties that are associated with releasing drugs in their active states are always issues for the conjugation strategy.[15] Furthermore, mAb–drug binding complexes have been generally constructed in a one-to-one ratio, which limits the tumor-killing potency. In contrast, the platinum(II)–Herceptin binding moieties that are formed primarily through metal complex coordination allow adjustable compound/mAb ratios to determine the appropriate number of molecules to attach to mAb to achieve a maximum effect.

The mechanism of Herceptin action is thought to involve many processes, including antibody-mediated cytotoxicity, receptor aggregation blocking, stimulation of Her2 endocytosis and removal of Her2 from the cell surface.[16,17] However, the underlying molecular mechanism for any form of mAb–platinum complexes requires further experimentation. The present results suggest that the Herceptin–Her2/neu surface binding is a key step for Her–$10L1Pt^{II}$ to exert its toxic functionality. The platinum(II)–Herceptin binding complex might be integrated by cells endocytotically, and then the parent toxic compounds are released from a lysosome, in which the proteolytic enzymes and the mild acidic condition (pH 5.5) brings about facile dissociation of the compound from Herceptin (Figure 8).[18] Alternatively, the complex moiety might release

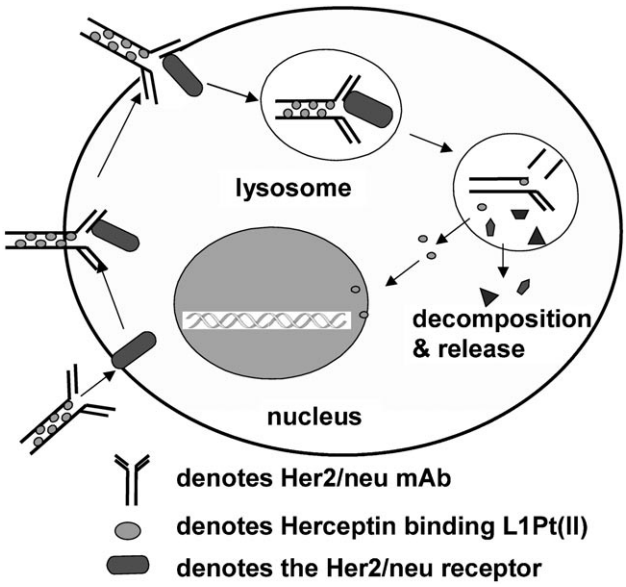

Figure 8. Mode of Herceptin access to the cell nucleus.

platinum compounds on the Her2/neu-binding site, and then the compounds pass through the cell membrane. Our apoptosis flow cytometry assay supports the first pathway. This seems to be reasonable given the fact that in low-Her2/neu-expressing MCF-7 cells, Her–$10L1Pt^{II}$ failed to induce significant apoptosis. Another consideration is that it is difficult for the parent cytotoxic molecules to dissociate from Herceptin on the cell surface, where the pH 7.4 condition is unfavorable. Additional biological studies are underway to fully understand the nature of this cancer-cell-specific agent. It is hoped that extensive application of this strategy in the treatment of human cancers will be developed in the near future.

Conclusions

In summary, a new type of platinum(II)–Herceptin complexes are described. They show specific cytotoxicity toward Her2/neu-overexpressing human cancer cells. The success of this approach depends largely on the binding ability of the Herceptin antibody to the platinum(II) compound, and its robustness in maintaining exquisite binding affinity toward Her2/neu. The remarkable cancer-cell-specific cytotoxicity of Her–10L1Pt^{II} in Her2-overexpressing SK-BR-3 cancer cells over normal cells has been demonstrated. It is shown that the L1Pt^{II}Cl$_2$ is an efficient regulator of cell apoptotic genes Bcl-2 and enhanced regulatory effects were observed in Her–10L1Pt^{II}-treated SK-BR-3 cells. The annexin V apoptosis assay demonstrates that Herceptin–Her2/neu surface binding is a key step in achieving the targeted effect. The chemical, cellular and molecular biological results of this study might open up a new therapeutic window into the development of a targeted protocol for the treatment of human cancers.

Experimental Section

Materials and measurements. All chemical reagents and solvents were of analytical grade and were obtained from Sigma–Aldrich. Methanol and acetonitrile were dried over molecular sieves (4 Å) prior to use. Analyses for C, H, and N were carried out on a Perkin-Elmer analyzer, model 240. Positive-ion ESI-MS data were recorded with an LCQ electrospray mass spectrometer. The spectra were recorded over the range *m/z* 200–1000.

Preparation of L1: A solution of 2-hydroxy-5-methylbenzaldehyde (0.20 mmol) was added dropwise to a solution that contained (*R*,*R*)-DACH (0.1 mmol) in EtOH (10 mL), then Et_3N (0.10 mmol) was added to the solution. After 2 h of stirring, a yellow-colored Schiff-base product was obtained. To this system was added solid $NaBH_4$ (80 mg, 0.2 mmol) to reduce the Schiff-base compound. The solution was magnetically stirred for an additional 2 h at room temperature. The solvent was removed by using a rotary evaporator. The reduced product was purified by column chromatography; yield: 95%. ^{1}H NMR ($CDCl_3$): $\delta = 1.29$–1.42 (m, 8H, CH_2 of *c*Hex), 2.36 (s, 6H, CH_3-phenol), 2.84 (s, 2H, CH of *c*Hex), 3.82 (m, 4H, CH_2-Ar), 6.52–6.83 ppm (m, 6H, Ar); ESI-MS: *m/z*: calcd for $C_{22}H_{30}N_2O_2$: 355.48 $[M+H]^+$, found: 355.42; elemental analysis calcd (%) for $C_{22}H_{30}N_2O_2$: C 74.54, H 8.53, N 7.90, found: C 74.4, H 8.6, N 8.0.

Preparation of L2: L2 was prepared and purified as described above for L1 with the exception that (*S*,*S*)-DACH was used; yield 92%. ^{1}H NMR ($CDCl_3$): $\delta = 1.29$–1.40 (m, 8H, CH_2 of *c*Hex), 2.35 (s, 6H, CH_3-phenol), 2.86 (s, 2H, CH of *c*Hex), 3.82 (m, 4H, CH_2-Ar), 6.55–6.82 ppm (m, 6H, Ar); ESI-MS: *m/z*: calcd (%) for $C_{22}H_{30}N_2O_2$: 355.48 $[M+H]^+$, found: 355.41; elemental analysis calcd (%) for $C_{22}H_{30}N_2O_2$: C 74.5, H 8.53, N 7.90, found: C 74.5, H 8.55 N 8.01.

Preparation of L3: L3 was prepared and purified as described above for L1 with the exception that (*R*,*S*)-DACH was used; yield 82%. ^{1}H NMR ($CDCl_3$): $\delta = 1.29$–1.42 (m, 8H, CH_2 of *c*Hex), 2.38 (s, 6H, CH_3-phenol), 2.89 (s, 2H, CH of *c*Hex), 3.95 (m, 4H, CH_2-Ar), 6.52–6.80 ppm (m, 6H, Ar); ESI-MS: *m/z*: calcd (%) for $C_{22}H_{30}N_2O_2$: 355.48 $[M+H]^+$, found: 355.50; elemental analysis calcd (%) for $C_{22}H_{30}N_2O_2$: C 74.5, H 8.53, N 7.90, found: C 74.2, H 8.61, N 7.92.

Preparation of L4: A solution of 3-formyl-4-hydroxybenzoic acid (0.20 mmol) was added dropwise to a solution that contained (*R*,*R*)-DACH (0.1 mmol) in EtOH (10 mL), then Et_3N (0.40 mmol) was added to the solution. After 2 h of stirring, a yellow-colored Schiff-base product was obtained. To this system was added solid $NaBH_4$ (0.2 m mol, 80 mg) to reduce the Schiff-base compound. The solution was magnetically stirred for an additional 2 h at room temperature. The solvent was removed by using a rotary evaporator. The reduced product was purified by column chromatography and was identified as the desired product; yield: 65%. ^{1}H NMR ($CDCl_3$): $\delta = 1.29$–1.39 (m, 8H, CH_2 of *c*Hex), 2.84 (s, 2H, CH of *c*Hex), 3.82 (m, 4H, CH_2-Ar), 6.82–7.79 ppm (m, 6H, Ar); ESI-MS: *m/z*: calcd (%) for $C_{22}H_{26}N_2O_6$: 415.45 $[M+H]^+$, found: 415.55; elemental analysis calcd (%) for $C_{22}H_{26}N_2O_6$: C 63.76, H 6.32, N 6.76, found: C 63.68, H 6.35, N 6.65.

Preparation of L1Pt^{II}Cl$_2$: A solution of compound L1 (0.2 mmol) in MeOH (5 mL) was added dropwise to an aqueous solution that contained the equivalent amount of K_2PtCl_4. Reaction at room temperature for 2 h resulted in the formation of a white precipitate; yield: 64%. ^{1}H NMR (D_2O): $\delta = 1.30$–1.39 (m, 8H, CH_2 of *c*Hex), 2.43 (s, 6H, CH_3-phenol), 2.88 (s, 2H, CH of *c*Hex), 3.62 (m, 4H, CH_2-Ar), 6.42–6.75 ppm (m, 6H, Ar); ^{195}Pt NMR ([D_7]DMF): $\delta = -2355$ ppm; ESI-MS: *m/z*: calcd (%) for $C_{22}H_{30}N_2O_2PtCl_2$: 621.47 $[M+H]^+$, found: 621.51; elemental analysis calcd (%) for $C_{22}H_{30}N_2O_2PtCl_2$: C 42.59, H 4.87, N 4.51, found: C 42.62, H 4.68, N 4.42.

Preparation of L2Pt^{II}Cl$_2$: A solution of compound L2 (0.2 mmol) in MeOH (5 mL) was added dropwise to an aqueous solution that contained the equivalent amount of K_2PtCl_4. Reaction at room temperature for 2 h resulted in the formation of a white precipitate; yield: 60%. ^{1}H NMR (D_2O): $\delta = 1.30$–1.38 (m, 8H, CH_2 of *c*Hex), 2.42 (s, 6H, CH_3-phenol), 2.82 (s, 2H, CH of *c*Hex), 3.66 (m, 4H, CH_2-Ar), 6.42–6.85 ppm (m, 6H, Ar); ^{195}Pt NMR ([D_7]DMF): $\delta = -2345$ ppm; ESI-MS: *m/z*: calcd (%) for $C_{22}H_{30}N_2O_2PtCl_2$: 621.47 $[M+H]^+$, found: 621.50; elemental analysis calcd (%) for $C_{22}H_{30}N_2O_2PtCl_2$: C 42.6, H 4.87, N 4.51, found: C 42.6, H 4.80, N 4.47.

Preparation of L3Pt^{II}Cl$_2$: A solution of compound L3 (0.2 mmol) in MeOH (5 mL) was added dropwise to an aqueous solution that contained the equivalent amount of K_2PtCl_4. Reaction at room temperature for 2 h resulted in the formation of a white precipitate; yield 42%. ^{1}H NMR (D_2O): $\delta = 1.25$–1.39 (m, 8H, CH_2 of *c*Hex), 2.45 (s, 6H, CH_3-phenol), 2.80 (s, 2H, CH of *c*Hex), 3.62 (m, 4H, CH_2-Ar), 6.40–6.85 ppm (m, 6H, Ar); ^{195}Pt NMR ([D_7]DMF): $\delta = -2352$ ppm; ESI-MS: *m/z*: calcd (%) for $C_{22}H_{30}N_2O_2PtCl_2$ 621.47 $[M+H]^+$, found: 621.48; elemental analysis calcd (%) for $C_{22}H_{30}N_2O_2PtCl_2$: C 42.6, H 4.87, N 4.51, found: C 42.4, H 4.64, N 4.37.

Preparation of L4Pt^{II}Cl$_2$: A solution of compound L4 (0.2 mmol) in MeOH (5 mL) was added dropwise to an aqueous solution that contained Et_3N (0.4 mmol) and K_2PtCl_4 (0.2 mmol). Reaction at room temperature for 2 h resulted in the formation of a white precipitate; yield 64%. ^{1}H NMR (D_2O): $\delta = 1.29$–1.39 (m, 8H, CH_2 of *c*Hex), 2.88 (s, 2H, CH of *c*Hex), 3.62 (m, 4H, CH_2-Ar), 6.66–7.76 ppm (m, 6H, Ar); ^{195}Pt NMR ([D_7]DMF): $\delta = -2352$ ppm; ESI-MS: *m/z*: calcd (%) for $C_{22}H_{26}N_2O_6PtCl_2$: 681.44 $[M+H]^+$, found 681.50; elemental analysis calcd (%) for $C_{22}H_{26}N_2O_6PtCl_2$: C 38.83, H 3.85, N 4.12, found: C 38.61, H 3.82, N 4.22.

Synthesis of L5: Compound L4 (0.2 mmol) was dissolved in MeOH (5 mL). 1,1′-Carbonyldiimidazole (CDI; 1 equiv) was added, and the mixture was stirred at room temperature for 2 h. To this system was added a THF solution that contained 5-carboxytetramethylrhodamine (0.2 mmol) with a hexanediamine-modified terminus. The reaction was carried out at room temperature and reached completion at 24 h, and the final product was purified by gel chromatography; yield 56%. ESI-MS: *m/z*: calcd (%) for $C_{53}H_{65}N_7O_7$ 913.13 $[M+H]^+$, found 913.12.

Synthesis of L5Pt^{II}Cl$_2$: A solution of compound L5 (0.2 mmol) in MeOH (5 mL) was added dropwise to an aqueous solution that contained an equivalent of K_2PtCl_4. After 2 h at room temperature a red-colored precipitate was isolated; yield 36%. ESI-MS: *m/z*: calcd (%) for $C_{53}H_{65}N_7O_7PtCl_2$: 1179.11 $[M+H]^+$, found: 1179.24.

Preparation of Herceptin–10L1Pt^{II} binding complex: An aqueous solution that contained Herceptin (175 mg, 1.0×10^{-3} mmol) was treated with an ethanolic solution of L1Pt^{II}Cl$_2$ (6.2 mg, 1.0×10^{-3} mmol). The resulting solution was homogeneous, and was allowed to stand at room temperature for 2 h. No precipitates formed. The binding complex solutions were filtered by size-exclusion chromatography (5000 Da). The filtrate was stored at 4 °C for future analysis. Herceptin–5L1Pt^{II} and Herceptin–L1Pt^{II} were prepared by using a similar procedure.

Preparation of Herceptin–10L5Pt^{II} binding complex: An aqueous solution that contained Herceptin (175 mg, 1.0×10^{-3} mmol) was treated with an ethanolic solution of L5Pt^{II}Cl$_2$ (11.8 mg, 1.0×10^{-3} mmol). The resulting solution was homogeneous and was allowed to stand at room temperature for 2 h. No precipitates formed. The binding complex solutions were filtered by size-exclusion chromatography (5000 Da), and the filtrate was stored at 4 °C for future analysis. Herceptin–5L5Pt^{II} and Herceptin–L5Pt^{II} were prepared by using a similar procedure.

Evaluation of the dissociation of Her–10L1Pt^{II} complex in acidic solution: A series of 0.1 mM aqueous solutions of Her–10L1Pt^{II} (10 mL) was treated with a small aliquot of 0.1 N HCl standard solution. The pH was adjusted to the desired value, which was monitored by a pH meter. Each of the resulting solutions (1 mL) were filtered by a size-exclusion column (10000 Da), and the filtrates were measured by UV/Vis.

Cell culture: Human cancer cell lines and wild-type fibroblast cells were obtained from American Type Culture Collection (ATCC, Manassas, VA, USA). Cells were maintained in an RPMI medium supplemented with 10% FBS, penicillin (100 μg mL^{-1}) and streptomycin (100 μg mL^{-1}) at 37 °C in an atmosphere that was humidified with 5% CO_2 and 95% air.

Growth inhibition assay: Cells were seeded in 96-well cell culture plates and treated on the second day with the experimental compounds. At the end of a two-day treatment, the cell number was estimated by sulforhodamine B (SRB) assay as described.[19] The percent growth inhibition was calculated by the following equation: % Inhibition $=(1-A_t/A_c)\,100$, for which A_t and A_c represent the absorbance in treated and control cultures, respectively.

Flow cytometric analysis: Apoptosis was determined by using the annexin V–FITC kit, by following the manufacturer's protocol (BD Pharmingen). Briefly, $\sim2\times10^6$ SK-BR-3 or MCF-7 cells were washed twice with cold PBS and then resuspended in 1× binding buffer at a concentration of 1×10^6 cells mL^{-1}. Then $\sim1\times10^5$ cells were stained by adding annexin V–FITC (5 μL) and propidium iodide (5 μL). The cells were gently vortexed and incubated for 15 min at room temperature in the dark. The addition of 1× binding buffer (400 μL) to each tube was followed by flow cytometry analysis within 1 h.

Real-time RT-PCR analysis: Total RNA from SK-BR-3 cancer cells was isolated with the Tri Reagent (Sigma, St. Louis, MO, USA). After DNA-free DNase treatment (Ambion, Austin, TX, USA), the total RNA (200 ng) was used in reverse transcription (RT) by the GeneAmp RNA PCR kit (PerkinElmer, Foster City, CA, USA). Real-time PCR was then performed on cDNA from reverse transcription reactions by using the OmniMix HS bead (Cepheid, Sunnyvale, CA, USA) according to the manufacturer's protocol. SYBR green dye (1×; Fisher Scientific, Atlanta, GA, USA) was added to the reaction mixture to detect amplicon synthesis in the SmartCycler real-time PCR thermal cycler (Cepheid, Sunnyvale, CA, USA). Specific primers of genes were designed on different exons, the following primers were used: Bcl-2: forward 5′-CAG CTG CAC CTG ACG CCC TTC ACC-3′, reverse 5′-CTG AGC AGA GTC TTC AGA GAC AGC-3′; Bcl-xL: forward 5′-GCA CTG TGC GTG GAA AGC GTA GAC-3′, reverse 5′-CTG AAG AGT GAG CCC AGC AGA ACC-3′. The specificity of the PCR-amplified product was verified by sequencing the product (data not shown). The thermal cycling conditions included an initial denaturation step at 95 °C for 2 min, and 45 cycles at 95 °C for 10 s, 65 °C for 15 s and 72 °C for 30 s. For quantification, the cycle threshold number (C_t) that exhibits the maximum curve growth rates was determined by using Cepheid SmartCycler software. The relative gene expression of each sample, which was normalized to that of glyceraldehyde-3-phosphate dehydrogenase (GAPDH), was calculated by using the formula: $2^{C_t(\mathrm{GAPDH})-C_t(\mathrm{gene})}$.

Acknowledgements

We are grateful to The Robert A. Welch Foundation for their award of grant A-084 that provided significant support for this research. This work was also supported by the NSF of China, 30672410, and the Guangdong Natural Science Foundation, 06104599.

Keywords: antibodies · apoptosis · cancer · Her2/neu · mRNA · platinum(II) compounds

[1] D. B. Shenoy, M. M. Amiji, *Int. J. Pharm.* **2005**, *293*, 261–270.
[2] K. Kataoka, A. Harada, Y. Nagasaki, *Adv. Drug Delivery Rev.* **2001**, *47*, 113–131.
[3] S. Sengupta, D. Eavarone, I. Capila, G. Zhao, N. Watson, T. Kiziltepe, R. Sasisekharan, *Nature* **2005**, *436*, 568–572.
[4] J. Kreuter, *Adv. Drug Delivery Rev.* **2001**, *47*, 65–81.
[5] S. Jaracz, J. Chen, L. V. Kuznetsova, I. Ojima, *Bioorg. Med. Chem.* **2005**, *13*, 5043–5054.
[6] R. V. Chari, *Adv. Drug Delivery Rev.* **1998**, *31*, 89–104.
[7] D. Schrama, R. A. Reisfeld, J. C. Becker, *Nat. Rev. Drug Discovery* **2006**, *5*, 147–159.
[8] A. M. Wu, P. D. Senter, *Nat. Biotechnol.* **2005**, *23*, 1137–1146.
[9] J. Chen, S. Jaracz, X. Zhao, S. Chen, I. Ojima, *Expert Opin. Drug Delivery* **2005**, *2*, 873–890.
[10] H. S. Cho, K. Mason, K. X. Ramyar, A. M. Stanley, S. B. Gabelli, D. W. Denney, D. J. Leahy, Jr., *Nature* **2003**, *421*, 756–760.
[11] N. E. Hynes, H. A. Lane, *Nat. Rev. Cancer* **2005**, *5*, 341–354.
[12] S. J. Chiu, N. T. Ueno, R. J. Lee, *J. Controlled Release* **2004**, *97*, 357–369.
[13] A. A. Bogan, K. S. Thorn, *J. Mol. Biol.* **1998**, *280*, 1–9.
[14] P. A. Trail, D. Willner, S. J. Lasch, A. J. Henderson, S. Hofstead, A. M. Casazza, R. A. Firestone, I. Hellstrom, K. E. Hellstrom, *Science* **1993**, *261*, 212–215.
[15] G. Payne, *Cancer Cell* **2003**, *3*, 207–212.
[16] D. Harari, Y. Yarden, *Oncogene* **2000**, *19*, 6102–6114.
[17] M. X. Sliwkowski, J. A. Lofgren, G. D. Lewis, T. E. Hotaling, B. M. Fendly, J. A. Fox, *Semin. Oncol.* **1999**, *26(4 Suppl. 12)*, 60–70.
[18] G. M. Dubowchik, M. A. Walker, *Pharmacol. Ther.* **1999**, *83*, 67–123.
[19] J. Gao, Y.-G. Liu, Y. Zhou, R. A. Zingaro, *ChemMedChem* **2007**, *2*, 1723–1729.

Received: December 7, 2007
Revised: February 4, 2008
Published online on March 25, 2008

